Influence of Core–Valence Separation of Electron Localization Function

MIROSLAV KOHOUT[1], ANDREAS SAVIN[2]

[1] *Institut für Theoretische Chemie, Universität Stuttgart, Pfaffenwaldring 55, 70569 Stuttgart, Germany*

[2] *Laboratoire de Chimie Théoretique (CNRS), Universite Pierre et Marie Curie, place Jussieu, F-75252 Paris Cedex 05, France*

Received 26 November 1995; accepted 16 December 1996

ABSTRACT: The electron localization function (ELF) shows too-high values when computed from valence densities only (instead of using the total density). This effect is mainly found when *d* electrons are present in the outermost shell of the core. Although no pronounced qualitative differences could be noticed in the examples studied up to now, it is found that the quantitative differences between the values of ELF obtained from the valence densities only or from the total densities can be large. We also show, for the first time, an example (the Be atom) where ELF is obtained directly from the density. This exemplifies the possibility of computing ELF from highly accurate calculations (or from experimental data). © 1997 John Wiley & Sons, Inc. *J Comput Chem* **18**: 1431–1439, 1997

Keywords: electron localization function; core–valence separation; *d* electrons; valence density; Pauh kinetic energy density

Introduction

A rough picture of the electron density of a molecule or solid is obtained by superimposing the atomic electron densities.[1,2] Each of the latter is a piecewise exponentially decaying function.[3] It is thus difficult to recognize at first sight the information about chemical bonding from a plot of the density, although all information about the molecular ground state should be present in the density.[4]

One possibility explored mainly by Bader and coworkers is to analyze the density derivatives.[5] Another very efficient way is to explicitly include effects due to the Pauli principle.[6,7] In our experience, the electron localization function of Becke and Edgecombe (ELF) proved to be very useful for describing different bonding situations.[7–10] In a density functional context, ELF can be defined as[9]:

$$\mathrm{ELF} = \frac{1}{1 + (t_P/t_{P,h})^2} \qquad (1)$$

Correspondence to: M. Kohout

CCC 0192-8651 / 97 / 121431-09

where:

$$t_P = \tau - \frac{1}{8}\frac{(\nabla\rho)^2}{\rho} \quad (2)$$

is the Pauli kinetic energy density of a closed shell system. $(\nabla\rho)^2/(8\rho)$ is the kinetic energy density of a bosonic-like system, where orbitals proportional to $\sqrt{\rho}$ are occupied.[11] t_P is always positive and, for an assembly of fermions, it describes the additional kinetic energy density required to satisfy the Pauli principle. The total electron density, ρ:

$$\rho = \sum_i^n |\psi_i|^2 \quad (3)$$

as well as the kinetic energy density:

$$\tau = \frac{1}{2}\sum_i^n |\nabla\psi_i|^2 \quad (4)$$

are computed from the orbitals, ψ_i. In both equations, the index i runs over all occupied orbitals. Using the homogeneous electron gas, we get, for the Pauli kinetic energy density, the value $t_{P,h}$, which is equal to $c_F\,\rho^{5/3}$ with the Fermi constant $c_F = \frac{3}{10}(3\pi^2)^{2/3}$.

ELF depends on the ratio $t_P/t_{P,h}$ as given by eq. (1). The Pauli kinetic energy density, t_P, does not mirror the ELF topology. This can be shown for the potassium atom (using Hartree–Fock orbitals obtained with the basis of Clementi and Roetti[12]). In this case, t_P is a monotonically decaying function, as can be seen in Figure 1. This monotonical decay of t_P is indeed very different from the ELF diagram (Fig. 2). The atomic shell

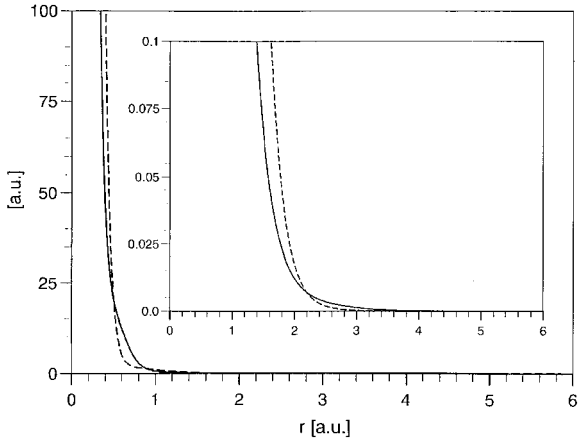

FIGURE 1. t_P (solid line) and $t_{P,h}$ (dashed line) for the potassium atom.

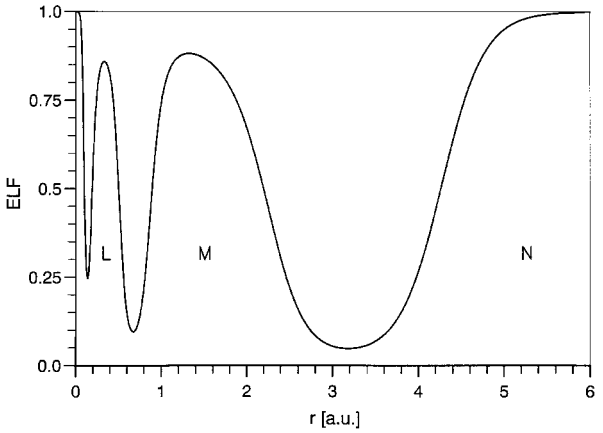

FIGURE 2. ELF for the potassium atom. The capital letters indicate the shells.

structure emerges after the comparision of t_P with $t_{P,h}$ as given by the ratio $t_P/t_{P,h}$ in the ELF formula. ELF takes values between 0 and 1. It reaches high values in the space regions where t_P is smaller than $t_{P,h}$ (cf. Figs. 1 and 2). The monotonical decay of t_P is found also for other atoms except of Li, Be, and B (cf. Figs. 3 and 4).

Although the electron density as well as the kinetic energy density are computed from the occupied orbitals, any unitary transformation of these occupied orbitals leaves both ρ and τ unchanged, and thus ELF is also unchanged.

ELF reveals the shell structure of atoms.[7,13] For an nth row atom there are n shells of high ELF values, separated from each other by regions of low ELF. In an ionic crystal, each atom is surrounded by the corresponding number of such nearly spherically symmetric shells. With decreasing ionic character of the bond the ELF region for

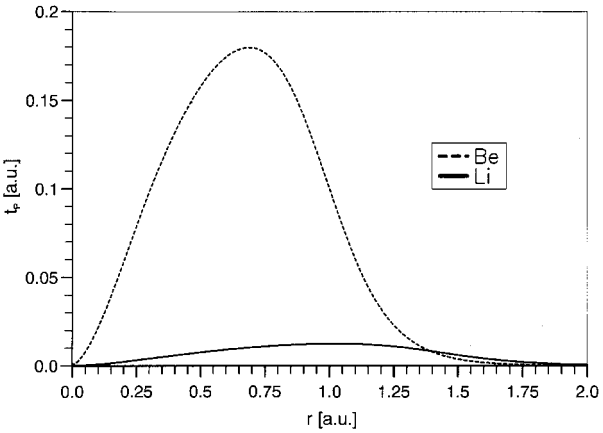

FIGURE 3. t_P for the Li and Be atom.

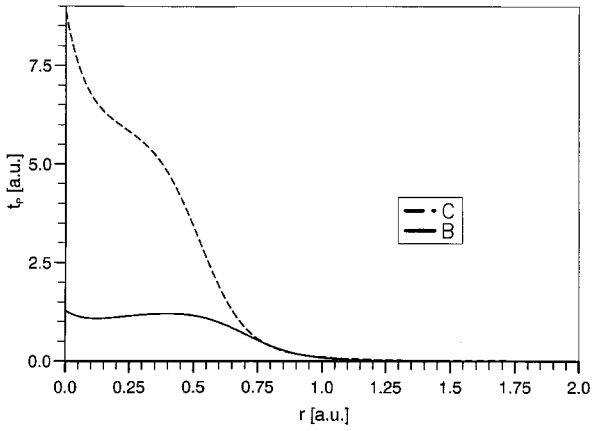

FIGURE 4. t_P for the B and C atom.

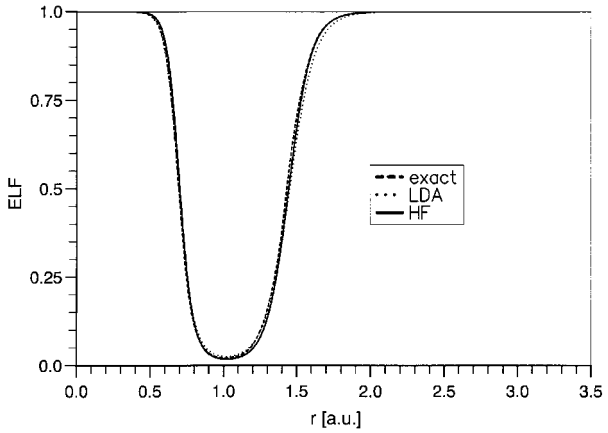

FIGURE 5. ELF for the Be atom. The "exact" ELF is computed from CI density; the LDA and HF values are given by the orbitals from the DF ADF program and the HF data of Clementi and Roetti,[12] respectively.

the valence shell of the electronegative element becomes more and more deformed. The values of high localization are concentrated between the bonded atoms. For a polar bond, those ELF regions are bent toward the more electronegative partner. A perfectly covalent bond is characterized by an ELF region of high localization symmetrically centered along the bond axis.[10]

In general, the orbitals appearing in the definition of ELF are those obtained from either Hartree–Fock (HF) or simplified Kohn–Sham-type (e.g., in the local density approximation, LDA) calculations. Is is important to stress that these can be seen as approximations to exact Kohn–Sham orbitals[14] that minimize the expectation value of the kinetic energy[15,16]:

$$T_s[\rho] = \min_{\Phi_D \to \rho} < \Phi_D | \hat{T} | \Phi_D > \qquad (5)$$

($T_s[\rho]$ is the kinetic energy of a noninteracting system with the electron density ρ, Φ_D a Slater determinant, and $\hat{T}$ the kinetic-energy operator).

The orbitals can be thus obtained directly from the density. This procedure requires a certain computational effort, but it allows one to obtain ELF from the electron density without any approximations. Of course, the generating density could be an experimental one. To illustrate this procedure, we used orbitals obtained from highest quality calculated densities.[17] The result for the Be atom is shown in Figure 5. It is clear that there is no noticeable difference between the "exact" ELF, and that obtained from HF or LDA. The HF orbitals are given by Clementi and Roetti,[12] whereas the LDA ones were obtained with the ADF program of Baerends et al.[18] using a double-zeta basis set.

Orbital Contributions to ELF

Following the formula for ELF [eq. (1)] we see that it is not possible to separate ELF into a valence and core part. Here, only the electron density and the kinetic energy density can be divided into the orbital contributions. But, this is no more possible for the Pauli kinetic energy, because of the term $\frac{1}{8}\frac{(\nabla\rho)^2}{\rho}$. Also, the ratio $t_P/t_{P,h}$ is not exactly separable into orbital contributions. Only if in the sum of orbital contributions to the electron density and its gradient some terms are negligibly small, is it possible to neglect these orbitals in the calculation of ELF. Thus, in the bond region, the valence ELF (computed from the valence density only) can be analyzed only if there is a clear separation between the core and valence density. Then the core density can be neglected and the valence ELF is practically identical with the all-electron ELF.

Traditionally, however, chemical properties are assigned to the valence regions. Many quantum chemical calculations carried out with pseudopotentials or with frozen core sustain this assumption by yielding good results for bond distances and atomization energies. We now ask about the possibility of using valence-only calculations also for analyzing their density; for example, for obtaining ELF. This can be studied by limiting the sums in eqs. (3) and (4) to the valence orbitals only (in case of pseudopotentials the valence orbitals are either

nodeless or exhibit fewer nodes than in an all-electron calculation).

Of course, no statement is made about the core region (orbitals from an all-electron and pseudopotential calculation differ mainly in this region), which can be considered unimportant. In the valence region, however, the core and valence orbitals can strongly overlap. From the formal point of view, we can expect good results from a valence-only approach only when both the valence and the core orbitals do not have large contributions in the same region of space. The amount to which one can expect such core-valence superposition is shown in two examples: Be and Zn.

In the valence-only calculation, the case of the Be atom is trivial. As the valence shell has only two electrons, ELF is equal to 1 everywhere as can be easily verified. When the total density is used, there are two electron pairs and therefore a clear minimum appears, corresponding to the separation between core and valence (see Fig. 5). After this minimum, ELF quickly reaches the value of 1, obtained also from valence-only calculation.

For Zn, a different picture is obtained (cf. Fig. 6—ELF computed from the HF data of Clementi and Roetti,[12] and an LDA calculation performed with ADF using the same basis set as valence functions). Whereas a two-electron pseudopotential would again yield a uniform value of 1, it can be seen that the all-electron ELF only slowly approaches this value in the outer atomic region. For a better understanding of this effect we will now turn to the contributions of different subshells to ELF, namely to the values obtained by limiting the summations appearing in eqs. (3) and (4) to the terms arising from a given subset of orbitals. ELF changes with the angular momentum of the subshell. A simplified argument can show that this change is related to the increase of the kinetic energy with angular momentum.

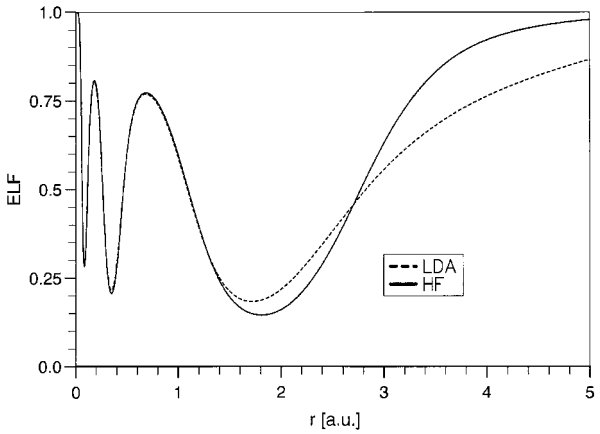

FIGURE 6. ELF for the Zn atom computed from the orbitals given by the DF ADF program and the HF data of Clementi and Roetti,[12] respectively.

Let us suppose Cartesian Slater functions of the form (like that utilized in the ADF program):

$$\psi_l = N_l x^i y^j z^k r^m e^{-\alpha_l r} \tag{6}$$

where N_l stands for the normalization constant:

$$N_l = \left[\frac{(2l+1)!!(2\alpha_l)^{2n+1}}{4\pi(2i-1)!!(2j-1)!!(2k-1)!!(2n)!} \right]^{1/2} \tag{7}$$

and $m = n - l - 1$ with the principal quantum number n and the orbital quantum number l.

When using only one Slater-type function for each orbital, the electronic density contribution, ρ_l, of a closed subshell with the orbital quantum number, l, is given [with $N(\alpha_l) = N_s^2$]:

$$\rho_l = 2(2l+1)N(\alpha_l) r^{2(n-1)} e^{-2\alpha_l r} \tag{8}$$

The kinetic energy density contribution, τ_l, and the quantity, $\frac{1}{8}\frac{(\nabla\rho_l)^2}{\rho_l}$, are:

$$\tau_l = (2l+1)N(\alpha_l) r^{2(n-2)} e^{-2\alpha_l r} \times \left[(n-1-\alpha_l r)^2 + l(l+1) \right] \tag{9}$$

$$\frac{1}{8}\frac{(\nabla\rho_l)^2}{\rho_l} = (2l+1)N(\alpha_l) r^{2(n-2)} e^{-2\alpha_l r} (n-1-\alpha_l r)^2 \tag{10}$$

Note that the last term appearing on the r.h.s. of eq. (9) will finally lead to an increase of the ratio $t_P/t_{P,h}$ (and the decrease of ELF) with l. For a fully occupied p or d subshell we get, with $t_{P,h} = c_F \rho_l^{5/3}$:

$$\frac{t_P}{t_{P,h}} = \frac{l(l+1)}{[(2l+1)N(\alpha_l)]^{2/3}} \frac{e^{\frac{4}{3}\alpha_l r}}{2^{5/3} c_F r^{\frac{2}{3}(2n+1)}} \tag{11}$$

For convenience, using the same exponent α for all orbitals, it is obvious that the ratio $t_P/t_{P,h}$ differs for various orbital quantum numbers l only by the factor $l(l+1)/(2l+1)^{2/3}$. This factor increases with increasing orbital quantum number. And, consistently, the ELF values for a d-subshell

are lower than the ones for a p-subshell with the same principal quantum number.

If the shell is built up from fully occupied orbitals with the same principal quantum number, n, but with different orbital quantum numbers, l_i, then the formula for the $t_P/t_{P,h}$ ratio is more complicated:

$$\frac{t_P}{t_{P,h}} = \frac{\Sigma_i l_i(l_i+1)(2l_i+1)N(\alpha_i)e^{-2\alpha_i r}}{\left[\Sigma_j(2l_j+1)N(\alpha_j)e^{-2\alpha_j r}\right]^{5/3}} \frac{1}{2^{5/3}c_F\, r^{\frac{2}{3}(2n+1)}} \tag{12}$$

To make the influence of the particular orbitals more evident, suppose all the orbitals have almost the same value for the exponents α_i and this is approaching the value of α. Near the ELF maximum the ELF value is almost independent of the exponents α_i. Then we can also take $e^{-2\alpha r}$ as well as $N(\alpha)$ for all orbitals. With those assumptions, $t_P/t_{P,h}$ can be written as:

$$\frac{t_P}{t_{P,h}} = \frac{1}{2^{5/3}c_F} \frac{\Sigma_i l_i(l_i+1)(2l_i+1)}{\left[\Sigma_j(2l_j+1)\right]^{5/3}} \left[\frac{e^{2\alpha r}}{N(\alpha)r^{(2n+1)}}\right]^{2/3} \tag{13}$$

The value of $t_P/t_{P,h}$ for the different combinations of orbitals is given by the l-dependent part of eq. (13). In the case of the s-, p-, and d- subshells we have foung the following: The addition of a subshell with an orbital quantum number higher than those already present in the atomic shell (e.g., adding a d-subshell to an s- or sp-subshell) increases the $t_P/t_{P,h}$ value (i.e., the ELF value decreases). The same is valid for the f-subshell with one exception. The combination of the d- and f-subshells has a higher ELF value than the d-subshell alone (on the condition that the orbital exponents are of the same magnitude for the two subshells).

The above theoretically derived behavior of ELF for different subshells can be studied with the case of an LDA calculation of the Zn atom (ADF program; the basis of Clementi and Roetti was used for the valence functions).

So, we find in Figure 7, where we depict the ELF for the subshell contributions in the M shell of the Zn atom, that the maximum for the $3d$ subshell, which only comes close to ELF = 0.3, is located underneath the $3p$ curve [cf. eq. (11)]. Of course, if the $3s$ orbitals were alone they would yield ELF = 1.

Further inspection of Figure 7 demonstrates ELF behavior in the case of a combination of fully occupied orbitals with various orbital quantum numbers l in the M-shell [cf. eq. (13)]. If the electron density is constructed from the $3s$ and $3p$ orbital densities, then the ELF maximum (the $3sp$ curve) is positioned above the $3p$ curve (i.e., between $3s$ and $3p$). Analogously, we can find the ELF maximum for the $3pd$ curve between the $3p$ and $3d$ maximum, and the one for the $3spd$ curve between the $3sp$ and $3d$ maximum. We state that a density contribution from orbitals with a higher orbital quantum number than is already available in the given shell produces a decrease in ELF.

This influence can propagate even in the next higher atomic shell. The $3s4s$ curve in Figure 8 was computed for the density constructed from the fully occupied $3s$ and $4s$ orbitals; it shows a sharp ELF increase in the N-shell. An addition of

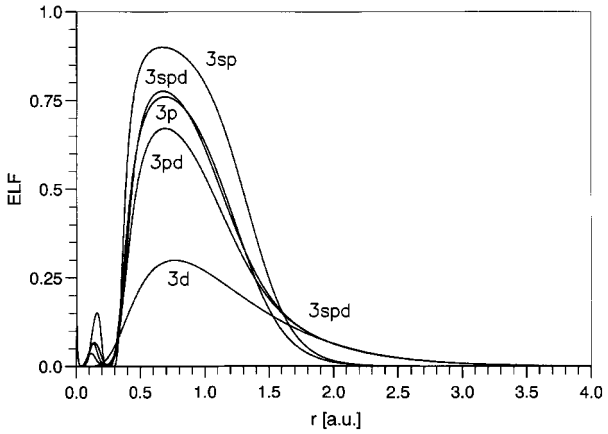

FIGURE 7. ELF for the density contributions in the M-shell of the Zn atom.

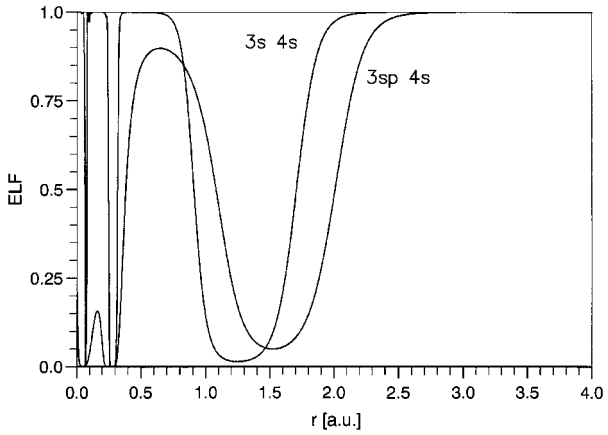

FIGURE 8. ELF for the Zn atom computed from the $3s$, $3p$, and $4s$ orbital densities.

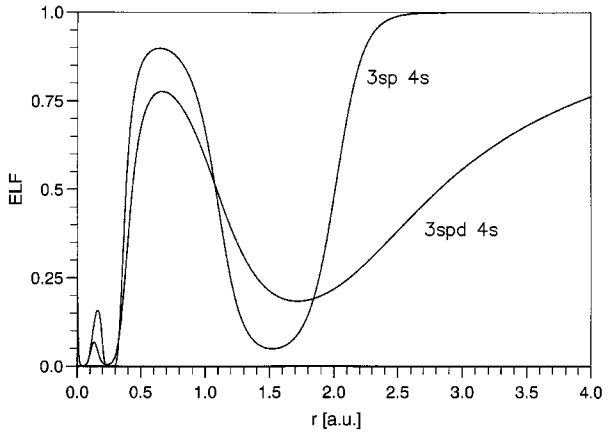

FIGURE 9. ELF for the M–N-shell of the Zn atom with and without the 3*d* orbital density.

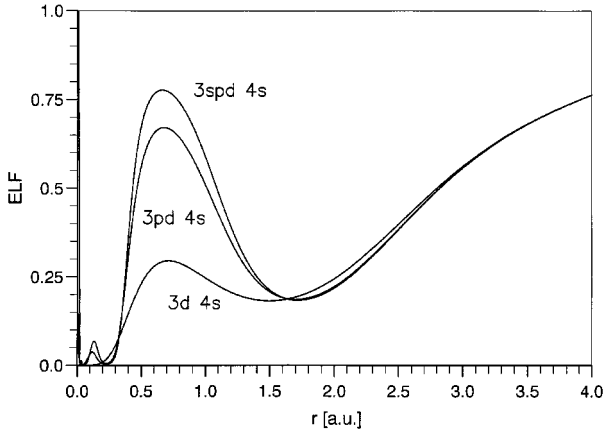

FIGURE 10. ELF for the M–N-shell of the Zn atom. Influence of the 3*s*, 3*p*, and 3*d* orbital densities on ELF in the valence region.

the 3*p* orbital density (the 3*sp*4*s* curve) results in a decrease of ELF in the N-shell of the Zn atom. However, due to the elimination of the 3*d*-subshell from the computation of ELF, a steep increase of ELF is still seen in the valence region (cf. also Fig. 9). The 3*spd*4*s* curve in Figure 9 shows the inclusion of the entire M-shell. There is, once again, a pronounced decrease of ELF in the valence shell. To make the picture complete we demonstrate that the decrease of ELF in the valence shell is due mainly to the influence of the 3*d* orbitals. In Figure 10, the 3*spd*4*s* curve resolves in the valence region ELF for the total density of the Zn atom. Calculation of ELF without the 3*s* or the 3*p* orbital density exhibits only a minute effect in the valence shell, as is manifested by the 3*pd*4*s* and 3*d*4*s* curve of Figure 10.

This shows that the lower value for the correct ELF compared to the one obtained from valence-only calculations is mainly due to the *d*-orbitals which penetrate the valence region. This effect has also been noticed for other quantities related to the analysis of electron density (see, e.g., refs. 19–22).

Examples and Results

The ELF representations of heavy metal compounds used earlier in the literature were computed from the valence density[8,10] (in the meantime, calculations with total density were also performed.[13,23] Both core (frozen core) and valence densities were obtained with the TB-LMTO program.[24] We chose, as a first example, the diamond structure of C, Si, Ge, and Sn (Fig. 11). All of these crystals are characterized by a covalent bond. Let us at first examine the second- and third-row compounds. As expected, the only difference between the total and valence representations is the evidence of the additional core shells (i.e., there is a hole in the core region for the valence-only diagrams). ELF undergoes only small changes in the valence region. From the element Scandium the 3*d* orbitals begin to fill up in the M shell. The same holds for the 4*d* orbitals in the penultimate shell of Yridium and so forth. Germanium possess 10*d* electrons in the penultimate shell. These fully occupied *d* orbitals penetrate the valence shell. It is now no longer possible to ignore the core density in the valence region. In this case, taking into account the core density results in a decrease of ELF in the valence region. For heavy metals the bond regions with high ELF values become smaller.

For all compounds in Figure 11, the valence diagrams exhibit high localization along the bond axis. This is indicative of a strong covalent bond. The inclusion of the core density produces a flattening of ELF in the bond region and thus a rather regular localization, especially for the compounds of the heavier atoms.

The penultimate-shell *d* electrons can produce considerable ELF diminution in the valence region. The examples of β-Sn (Fig. 12) illustrates how deep ELF can drop in the bond region (from the value of 0.7 to 0.4), if the core density is taken into consideration.

For this compound there is large penetration of *d*-subshell electrons into the valence shell. In this case, the core density cannot simply be neglected in the valence region. Indeed, the ELF computed from the total density differs substantially from

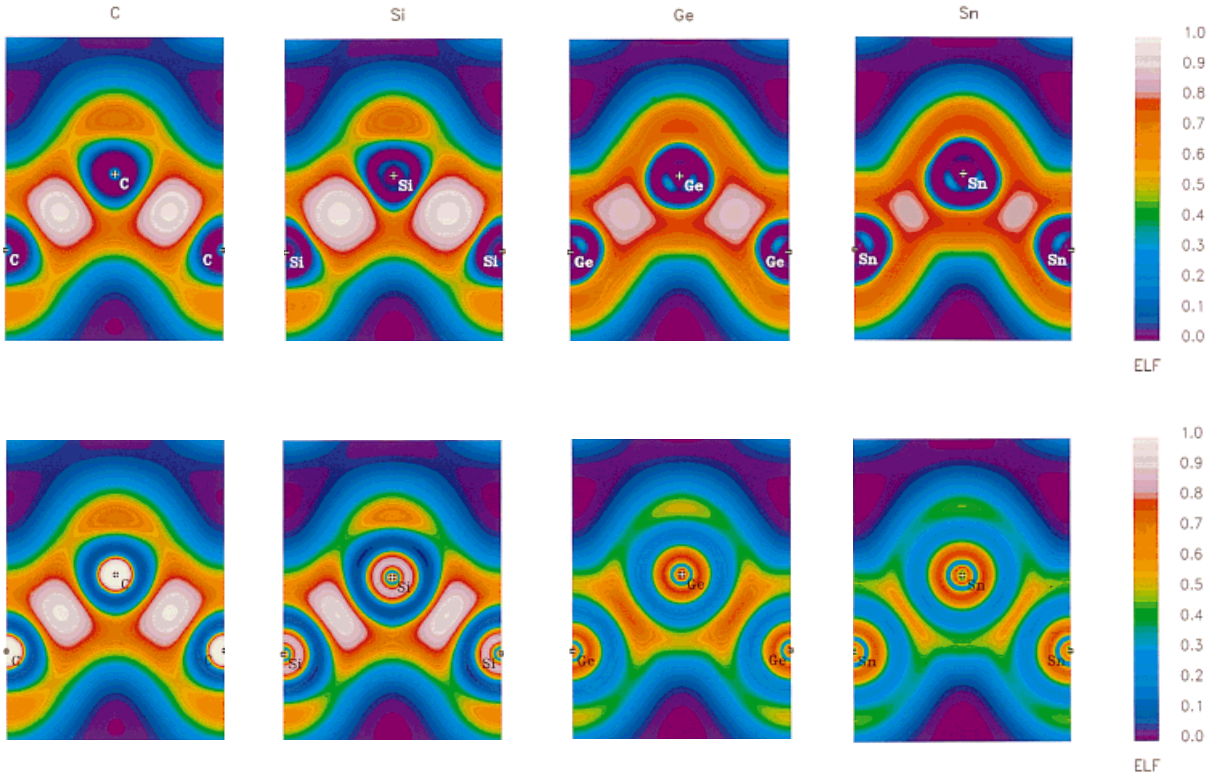

FIGURE 11. ELF for the diamond structure of C, Si, Ge, and Sn. The figures in the upper row are computed from the valence density, in the lower row from the total density.

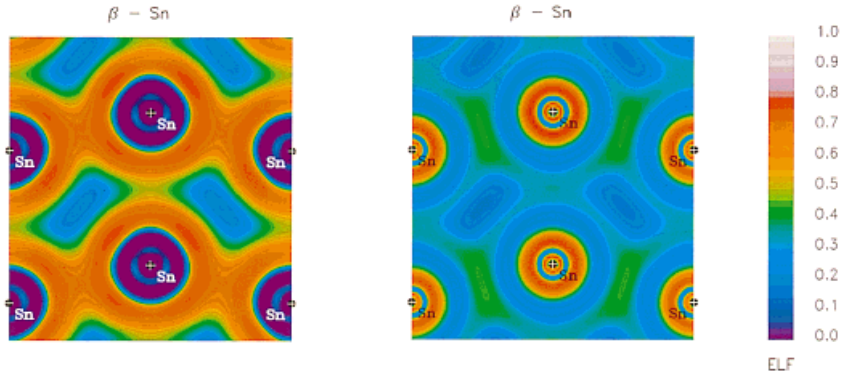

FIGURE 12. ELF for the β-Sn computed from the valence density (left) and the total density (right).

the valence ELF (i.e., ELF computed from the valence density only). Close inspection of Figure 12 reveals a somewhat higher localization along the bond axis; that is, a partially covalent character. Besides ELF magnitude, the general distribution of the localization is also very important.

In Figure 13 we present diagrams for the binary III–V compounds in the sphalerite structure. Going from the valence to the total density the aforementioned changes in ELF also hold for these polar compounds. The reduction of the high ELF magnitude bond regions is, in the case of BN, negligible, but is evident for AlP, although still relatively small. In the bond regions of the compounds GaAs and InSb, ELF drops to a value of about 0.7 and these regions are formed in narrow areas bent in the direction of the anion. This effect of the *d* electrons can be noticed even if only one

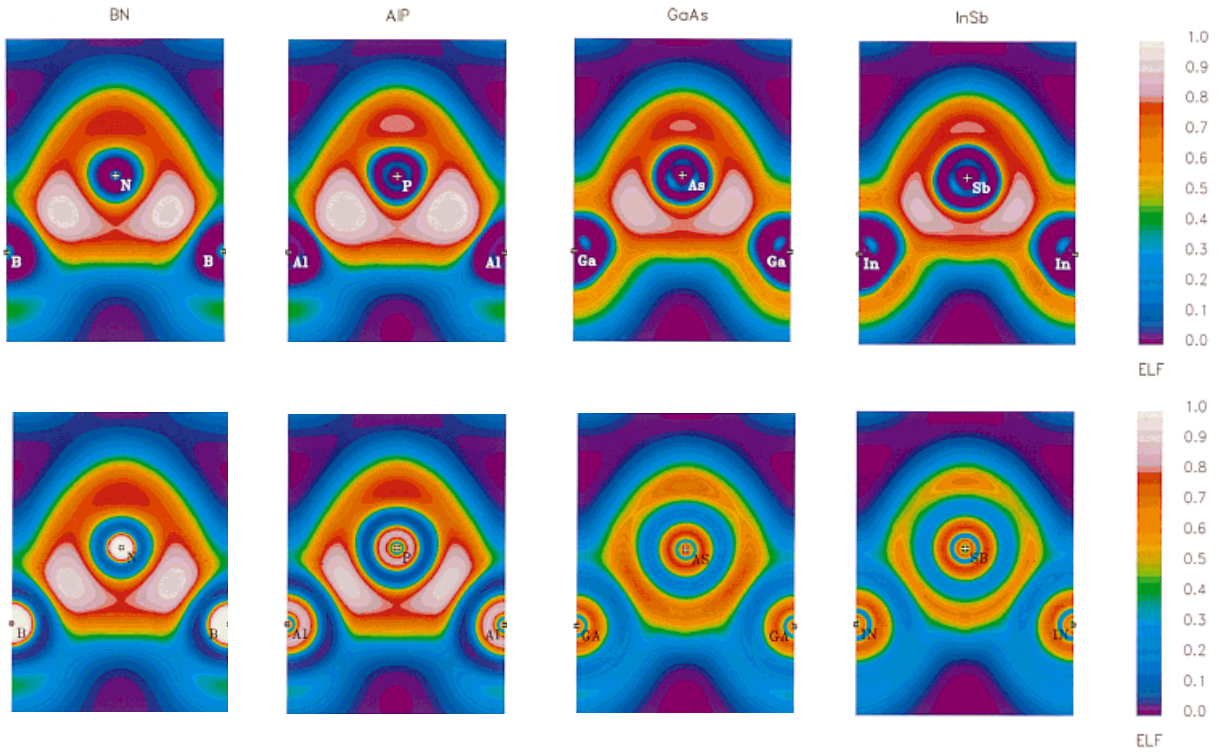

FIGURE 13. ELF for the binary III–V compounds in the sphalerite structure computed from the valence density (upper row), and the total density (lower row).

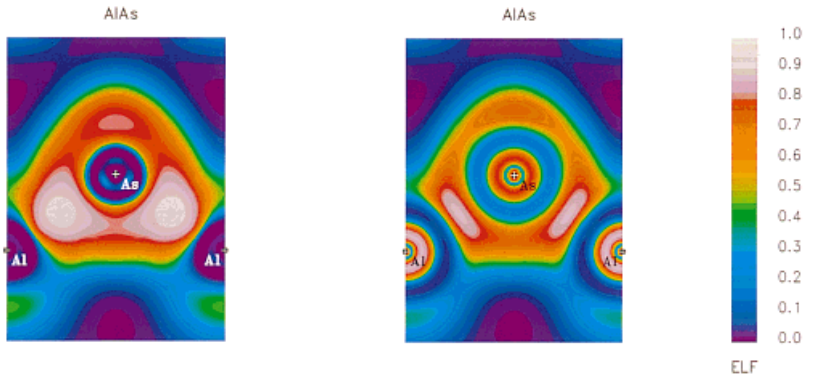

FIGURE 14. ELF for the sphalerite structure of AlAs computed from the valence density (left) and the total density (right).

of the participant elements possesses occupied *d* orbitals. Computing ELF from the valence density of AlAs (Fig. 14) we find a large area of high-magnitude ELF along the bond axis. Taking into account the core densities results in shrinking of these regions, although not to such an extent as in case of GaAs.

Conclusions

ELF has proven to be a useful tool in the characterization of chemical bonding. Care is recommended, however, when valence-only results are used to produce ELF. In particular, the *d*-subshell

tends to penetrate the valence region and its exclusion produces values for ELF that are too high when compared with those obtained from all-electron calculations.

We have also shown that it is possible to produce ELF by using only electron densities. This procedure shows that it is possible to use experimentally accessible data for generating ELF plots.

Acknowledgment

The authors thank Prof. E. J. Baerends (Vrije Universiteit, Amsterdam) for making available the density-functional program, ADF; Prof. V. H. Smith, Jr. (Queen's University, Kingston) for reading the manuscript; and Prof. B. Silvi (Universite Pierre et Marie Curie, Paris) and Prof. H. G. von Schnering (Max-Planck-Institut für Festkörperforschung, Stuttgart) for stimulating discussions.

References

1. M. Roux, S. Besnainou, and R. Daudel, *J. Chim. Phys.*, **54,** 218 (1956).
2. R. F. W. Bader, W. H. Henneker, and P. E. Cade, *J. Chem. Phys.*, **46,** 3341 (1967).
3. W.-P. Wang and R. G. Parr, *Phys. Rev. A*, **16,** 891 (1977).
4. P. Hohenberg and W. Kohn, *Phys. Rev. B*, **136,** 864 (1964).
5. R. F. W. Bader, *Atoms in Molecules, a Quantum Theory*, Clarendon Press, Oxford, 1990.
6. W. L. Luken and J. C. Culberson, *Int. J. Quant. Chem.*, **16,** 265 (1982).
7. A. D. Becke and K. E. Edgecombe, *J. Chem. Phys.*, **92,** 5397 (1990).
8. A. Savin, A. D. Becke, J. Flad, R. Nesper, H. Preuss, and H. G. von Schnering, *Angew. Chem. Int. Ed. Engl.*, **30,** 409 (1991).
9. A. Savin, O. Jepsen, J. Flad, O. K. Andersen, H. Preuss, and H. G. von Schnering, *Angew. Chem.*, **104,** 186 (1992).
10. M. Kohout, A. Savin, J. Flad, H. Preuss, and H. G. von Schnering, in *Computer Aided Innovation of New Materials II*, M. Doyama, J. Kihara, M. Tanaka, and R. Yamamoto, Eds., Elsevier, Amsterdam, 1993, pp. 201–203.
11. Y. Tal and R. F. W. Bader, *Int. J. Quant. Chem. Quant. Chem. Symp.*, **12,** 153 (1978).
12. E. Clementi and C. Roetti, *Atom. Data Nucl. Data Tables*, **14,** 218 (1974).
13. M. Kohout and A. Savin, *Int. J. Quant. Chem.*, **60,** 875 (1996).
14. W. Kohn and L. J. Sham, *Phys. Rev. A*, **140,** 1133 (1965).
15. M. Levy, *Proc. Natl. Acad. Sci. USA*, **76,** 6062 (1979).
16. J. P. Perdew and A. Zunger, *Phys. Rev. B*, **23,** 5048 (1981).
17. Q. Zhao and R. G. Parr, *Phys. Rev. A*, **46,** 2337 (1992).
18. E. J. Baerends, D. E. Ellis, and P. Ros, *Chem. Phys.*, **2,** 41 (1973); G. te Velde and E. J. Baerends, *J. Comput. Phys.*, **99,** 6109 (1992).
19. Z. Shi and R. J. Boyd, *J. Chem. Phys.*, **88,** 4375 (1988).
20. R. P. Sagar, A. C. T. Ku, V. H. Smith Jr., and A. M. Simas, *J. Chem. Phys.*, **88,** 4367 (1988).
21. R. P. Sagar, A. C. T. Ku, V. H. Smith Jr., and A. M. Simas, *Can. J. Chem.*, **66,** 1005 (1988).
22. M. Kohout, A. Savin, and H. Preuss, *J. Chem. Phys.*, **95,** 1928 (1991).
23. U. Häussermann, S. Wengert, P. Hoffman, A. Savin, O. Jepsen, and R. Nesper, *Angew. Chem.*, **106,** 2147 (1994).
24. M. van Schilfgaarde, T. A. Paxton, O. Jepsen, and O. K. Andersen, TB-LMTO Program.